Journal of Experimental Botany
https://doi.org/10.1093/jxb/erad439 Advance Access Publication 3 November 2023

RESEARCH PAPER

Role of transcription factor complex OsbHLH156–OsIRO2 in regulating manganese, copper, and zinc transporters in rice

Jiamei Zhu[1,†], Jie Li[1,†], Xiaoying Hu[1], Jin Wang[1], Jing Fang[1], Shoudong Wang[2,3,*], and Huixia Shou[1,3,*]

[1] State Key Laboratory of Plant Physiology and Biochemistry, College of Life Sciences, Zhejiang University, Hangzhou, Zhejiang 310058, China
[2] Key Laboratory of Soybean Molecular Design Breeding, Northeast Institute of Geography and Agroecology, Chinese Academy of Sciences, Changchun 130102, China
[3] Zhejiang Lab, Hangzhou 310012, China

[†] These authors contributed equally to this work.
[*] Correspondence: huixia@zju.edu.cn or wangshoudong@iga.ac.cn

Received 10 May 2023; Editorial decision 26 October 2023; Accepted 2 November 2023

Editor: Anne Krapp, INRAE, France

Abstract

Iron (Fe), manganese (Mn), copper (Cu), and zinc (Zn) are essential micronutrients that are necessary for plant growth and development, but can be toxic at supra-optimal levels. Plants have evolved a complex homeostasis network that includes uptake, transport, and storage of these metals. It was shown that the transcription factor (TF) complex OsbHLH156–OsIRO2 is activated under Fe deficient conditions and acts as a central regulator on Strategy II Fe acquisition. In this study, the role of the TF complex on Mn, Cu, and Zn uptake was evaluated. While Fe deficiency led to significant increases in shoot Mn, Cu, and Zn concentrations, the increases of these divalent metal concentrations were significantly suppressed in *osbhlh156* and *osiro2* mutants, suggesting that the TF complex plays roles on Mn, Cu, and Zn uptake and transport. An RNA-sequencing assay showed that the genes associated with Mn, Cu, and Zn uptake and transport were significantly suppressed in the *osbhlh156* and *osiro2* mutants. Transcriptional activation assays demonstrated that the TF complex could directly bind to the promoters of *OsIRT1*, *OsYSL15*, *OsNRAMP6*, *OsHMA2*, *OsCOPT1/7*, and *OsZIP5/9/10*, and activate their expression. In addition, the TF complex is required to activate the expression of nicotianamine (NA) and 2'-deoxymugineic acid (DMA) synthesis genes, which in turn facilitate the uptake and transport of Mn, Cu, and Zn. Furthermore, OsbHLH156 and OsIRO2 promote Cu accumulation to partially restore the Fe-deficiency symptoms. Taken together, OsbHLH156 and OsIRO2 TF function as core regulators not only in Fe homeostasis, but also in Mn, Cu, and Zn accumulation.

Keywords: Crosstalk, iron deficiency, micronutrients, *Oryza sativa*, OsbHLH156, OsIRO2.

Introduction

Micronutrients like iron (Fe), manganese (Mn), copper (Cu), and zinc (Zn) are essential elements that must be precisely maintained within small concentration ranges for healthy plant growth and development. Deficiency or excess of any of these

metals cause serious damage to plant physiological and biochemical processes (Alejandro *et al.*, 2020; Bashir *et al.*, 2021; Zahra *et al.*, 2021; Kirk *et al.*, 2022). Hence, the sensing, signalling, and transport of Fe, Mn, Cu, and Zn as well as crosstalk among the mechanisms maintaining these nutrient levels need to be precisely regulated. Studies have shown that these metals affect the homeostasis of each other in plant tissues (Rout *et al.*, 2015; Bashir *et al.*, 2016). In particular, Fe deficiency can dramatically adjust uptake and transport of the other three elements in both monocotyledonous and dicotyledonous species. Fe is involved in many of the same biological processes as Mn, Cu, or Zn, i.e. chlorophyll synthesis and photosynthesis (Fe, Mn, and Cu), mitochondrial respiration (Fe, Mn, and Cu), oxidative stress protection (Fe, Mn, Cu, and Zn), nitrogen metabolism (Fe, Mn, and Cu), and pathogen defence (Fe and Cu), as well as serving as enzyme cofactors (Fe, Mn, Cu, and Zn) (Hansch and Mendel, 2009; Zhao *et al.*, 2012; Kobayashi *et al.*, 2019). However, the molecular mechanisms underlying Fe homeostasis and its crosstalk with Mn, Cu, and Zn levels are not fully understood.

Although Fe is abundant in the soil, plants are still at risk of Fe deficiency, because most iron exists in the form of insoluble ferric hydroxides, which largely reduce the efficiency of Fe utilization. To cope with this issue, plants have evolved two Fe acquisition strategies: the reduction strategy (Strategy I), in non-gramineous plants like *Arabidopsis*, and the chelation strategy (Strategy II), in gramineous plants like rice (Kobayashi and Nishizawa, 2012; Kobayashi *et al.*, 2014, 2019). Plants acquire Fe through three steps using Strategy I: firstly, the root cells secret phenolic compounds and protons to mobilize Fe, making the ferric Fe more soluble (Santi *et al.*, 2005), then the enzyme FRO2 reduces Fe(III) to Fe(II) (Robinson *et al.*, 1999; Connolly *et al.*, 2003), and finally the Fe(II) is transported into a cell by the IRON-REGULATED TRANSPORTER 1 (IRT1) (Korshunova *et al.*, 1999;Vert *et al.*, 2002). For Strategy II plants, mugineic acid family phytosiderophores (MAs) are secreted into the rhizosphere to chelate the Fe(III) through TOM1 (Transporter of mugineic acid family phytosiderophores 1) (Ma and Nomoto, 1993; Ma *et al.*, 1995; Nozoye *et al.*, 2011), and the chelates [Fe(III)-MA] are then transported into the cell by the YELLOW STRIPE-LIKE transporter (YSL) (Curie *et al.*, 2001; Inoue *et al.*, 2009). After uptake by the root, iron is first transported from the epidermal cells to the vascular bundle via symplastic and apoplastic routes that bring it through the Casparian strip, and it is then translocated from root to shoot via xylem or phloem loading (Kobayashi and Nishizawa, 2012; Kobayashi *et al.*, 2019). In the plant body, both Fe(II) and Fe(III) must be chelated because of the serious toxicity of soluble Fe(II) and low solubility of Fe(III). One important metal chelator for facilitating transport of Fe(II) and other transition metals inside plants is NA, which is synthesized by three NA synthases, OsNAS1, OsNAS2, and OsNAS3 (Inoue *et al.*, 2003). DMA is a structural analogue of NA that is synthesized from NA by nicotianamine aminotransferase (NAAT) and deoxymugineic acid synthase (DMAS). DMA has been detected in rice xylem and phloem saps as a chelator of Fe(III) (Mori *et al.*, 1991).

Fe deficiency increases the accumulation of other divalent metals like Mn, Cu, and Zn in *Arabidopsis* and rice (Cheng *et al.*, 2007; Long *et al.*, 2010; Waters *et al.*, 2012; Barberon *et al.*, 2014; Cai *et al.*, 2021). On the one hand, the low selectivity of some universal metal transporters could also transport other divalent metals. AtIRT1 could transport non-Fe metals such as Zn, Mn, cobalt (Co), or cadmium (Cd) (Rogers *et al.*, 2000;Vert *et al.*, 2002) and AtNRAMP1 could also transport Mn and Cd besides iron (Curie *et al.*, 2000; Thomine *et al.*, 2000; Cailliatte *et al.*, 2010). On the other hand, many non-Fe metal transporters were found to be induced by Fe deficiency stress. Expression of the Cu-uptake genes *AtCOPT2*, *AtFRO4*, and *AtFRO5* were up-regulated by AtFIT (Fer-Like Iron Deficiency-Induced Transcription Factor) under Fe deficiency (Cai *et al.*, 2021). *AtMTP8* (*Metal Tolerance Protein 8*) is strongly induced in low-Fe conditions, and plays an important role in preventing the antagonistic interference of Mn with Fe nutrition in *Arabidopsis* (Eroglu *et al.*, 2015). AtMTP3 was found to mediate Zn exclusion from the shoot under Fe deficiency (Arrivault *et al.*, 2006). AtIREG2 (Iron-regulated membrane protein 2) is also induced by Fe deficiency stress, which localized to the tonoplast and sequestered nickel (Ni), Fe, and Co to the vacuoles (Schaaf *et al.*, 2006; Morrissey *et al.*, 2009).

Recently, the basic helix-loop-helix (bHLH) TF OsbHLH156 was found to physically interact with the major regulator OsIRO2 (Ogo *et al.*, 2006, 2007) and facilitates its nuclear localization to regulate expression of Strategy II genes during Fe deficiency in rice (Wang *et al.*, 2020). A separate group named *OsbHLH156* as *OsFIT* for its sequence similarity to *Arabidopsis FIT* (Liang *et al.*, 2020). When lacking either *OsbHLH156/OsFIT* or *OsIRO2*, rice plants cannot synthesize mugineic acid (MA) and take up Fe(III) through Fe(III)-MA complexes. On the other hand, the Fe deficiency induced Fe(II) transporters OsIRT2 and OsNRAMP1 are not regulated by the TF complex, while OsIRT1 is only partially regulated. Therefore, the mutant did not show significant chlorosis symptoms when Fe(II) was supplied as it can take up Fe(II) through OsIRT1, OsIRT2, and OsNRAMP1 (Wang *et al.*, 2020). However, whether and how *OsbHLH156* and *OsIRO2* regulate the uptake and transport of Mn, Cu, and Zn are unclear. In this study, we show that OsbHLH156 and OsIRO2 directly bind to the promoters of genes associated with Fe, Mn, Cu, and Zn uptake and transport as well as NA synthesis genes and activate their expression to modulate Fe crosstalk with Mn, Cu, and Zn in rice.

Materials and methods

Plant materials and growth conditions

The cultivars Nipponbare (Nip) and Zhonghua No. 11 (ZH11) of *Oryza sativa* L. subsp. *japonica* were used as the wild type (WT) control in this

study. The mutant *osbhlh156-1* (Nip background) has been described previously (Wang *et al.*, 2020). All plants were grown in a growth chamber under 16/8 h light/dark cycles, 500 μmol m^{-2} s^{-1} light intensity, and 30/25 °C. The hydroponic and pot experiments were conducted as described previously (Wang *et al.*, 2020). Briefly, germinated seeds were placed on a net floating on a nutrient solution containing 1.43 mM NH_4NO_3, 0.32 mM NaH_2PO_4, 0.51 mM K_2SO_4, 1.0 mM $CaCl_2$, 1.64 mM $MgSO_4$, 0.25 mM Na_2SiO_3, 9 μM $MnCl_2$, 0.13 μM $CuSO_4$, 0.08 μM $(NH_4)_6Mo_7O_{24}$, 0.02 μM H_3BO_3, 0.15 μM $ZnSO_4$, and ethylenediamine tetraacetic acid (EDTA)-Fe(II) (0 or 125 μM) and adjusted to pH 5.5–5.6. For pot experiments, dry soil was put into pots, watered with tap water, and kept either moist or submerged for more than 1 month to prepare the simulated upland and flooded conditions, respectively. After that, 7-day-old seedlings (WT, *osbhlh156*, and *osiro2*) grown under Fe-supplied conditions were transferred to upland and flooded pots for 1 month. For time-course analysis, 1-week-old seedlings (WT) grown under Fe-supplied conditions were exposed to Fe-deficiency nutrient solution for 7 d and then returned to Fe-supplied conditions for 3 d. The root tissues were collected after 0, 1, 3, 4, 5, and 7 d under Fe deficiency or 1, 2, and 3 d after resupplying Fe to Fe-deficient plants.

Plasmid construction for plant transformation

To generate CRISPR/Cas9 constructs targeting *OsbHLH156* and *OsIRO2*, 20-bp target sequences of 5'-TGTCGGCGGCGACTGGATGG-3' in the first exon of *OsbHLH156* and 5'-GGTCTTGGACATCGTCGTCG-3' in the first exon of *OsIRO2* were used to design gRNA spacers and cloned into pRGE31 (Addgene, MA, USA) (Wang *et al.*, 2020). To analyse the subcellular localization of OsIRO2 *in vivo*, a 3844-bp genomic fragment of *IRO2*, containing the 1669-bp promoter (upstream of ATG) and the entire 2175-bp coding region without a stop codon was amplified from Nip genomic DNA, fused to N-terminus of *mCherry*, and cloned into the vector pTF101. The vector was named *pOsIRO2:gOsIRO2-mCherry*. The above binary vectors were introduced into *Agrobacterium* strain EHA101 or EHA105 for rice transformation using callus derived from mature seeds of WT via *Agrobacterium*-mediated transformation as described previously (Chen *et al.*, 2003).

Mutant identification

In order to obtain *osbhlh156* and *osiro2* homozygous mutants generated by CRISPR/Cas9, detection primers (Supplementary Table S1) upstream and downstream of the target site of OsbHLH156 and OsIRO2 were designed, respectively. After amplification, the resulting products were detected using first-generation sequencing by the sequencing company Sangon Biotech (Shanghai, China) for screening *osbhlh156* and *osiro2* homozygous mutants.

Soil Plant Analysis Development measurement

The middle regions of the youngest fully expanded leaves were selected to measure the Soil Plant Analysis Development (SPAD) value using a portable chlorophyll meter (SPAD-502; Konica Minolta Sensing, Japan). Each leaf was measured three times, the average of the values was counted as one biological replicate.

Transcriptome analysis

Sample collection, RNA extraction, and transcriptome analysis were conducted as previously described (Wang *et al.*, 2020). WT, *osbhlh156*, and *osiro2* mutants were grown in hydroponic conditions with or without Fe for 10 d, the shoots and roots from three plants were harvested as one biological replicate for RNA extraction. Three independent biological replicates were used for each sample. Paired-end sequencing was performed on a BGISEQ-500 sequencer (BGI, Shenzhen, China) following the recommended protocol. Differentially expressed genes (DEGs) between samples were detected using DESEQ2. The cutoff value, fragments per kilobase of transcript per million mapped reads (FPKM) >10, $\log_2$(fold change) >1 or <−1 with $P<0.05$, was used for DEG analysis.

RNA extraction and RT–qPCR

The samples collected from roots or leaves were ground in liquid nitrogen with a tissue homogenizer (TL2010S; DHS, China). Total RNA extraction and RT–qPCR were performed as previously reported (Wang *et al.*, 2020). First-strand cDNA synthesis was performed with a cDNA Synthesis Kit (TaKaRa, Dalian, China). RT–qPCR was conducted using SYBR premix ExTaq (TaKaRa). *OsACTIN1* (LOC_Os03g50885) was used as an internal control. Transcript levels were calculated relative to *OsACTIN1* using the Equation $2^{-\Delta Ct}$. Another housekeeping gene, ubiquitin (UBQ, LOC_Os01g22490), was used to verify the consistent expression of *OsACTIN1* under the different growth conditions used in this study. All amplification reactions were performed with three biological replicates and two technical replicates. Primers used for qRT-PCR are listed in Supplementary Table S1.

NA and DMA contents

Seeds of the WT, *osbhlh156*, and *osiro2* were germinated and grown on nutrient solution without Fe for 10 d. Extraction and quantification of NA and DMA were carried out as described with some modifications (Cheng *et al.*, 2007). To determine the NA content, root tissues were collected and ground into powder in liquid nitrogen, then 300 μl deionized water was added for extraction at 80 °C for 30 min. After centrifugation, the supernatant was used for NA quantification using an Agilent 6460 series liquid chromatography-mass spectrometry (LC-MS) (Palo Alto, CA, USA). For DMA secretion analysis, 10-day-old WT, *osbhlh156*, and *osiro2* seedlings grown under Fe deficiency were transferred to deionized water (10 ml) in 15 ml tubes after 2 h of illumination in the greenhouse, with each line sampled in three replicate tubes. After dipping in deionized water for 5 h, the water samples were collected and filtered through a 0.22 μm membrane filter to remove the root residues in the water. The filtered water samples were frozen and dried using a lyophilizer (Zirbus VaCo2, Zirbus Technology, Germany), and then re-dissolved by adding 1 ml deionized water. The liquid was used for DMA detection using an Agilent 6460 series LC-MS. NA and DMA had peak retention times at 1.80 min and 1.95 min, respectively. Quantification of NA and DMA were based on the LC-MS peak area, and a calibration curve constructed by quantifying peak areas of the standard in seven different concentrations (3.2–2000 ng ml^{-1}). The 304 to 185 m/z and 303 to 187 m/z daughter transitions were used to quantify NA and DMA, respectively.

Measurement of elements

Element concentrations were determined as described previously (Wang *et al.*, 2020). Shoots samples were dried for 3 d at 70 °C and then digested in 5 ml 11 M HNO_3 and 1 ml 30% H_2O_2 for 30 min at 190 °C. Concentrations of the elements were measured using inductively coupled plasma mass spectrometry (ICP-MS; Agilent 7500ce).

Yeast two-hybrid assay

The coding sequences (CDS) of *OsbHLH156* and *OsIRO2*, amplified from cDNA, were cloned into the pGADT7-Rec vector to generate pGAD-Preys (AD-OsbHLH156 and AD-OsIRO2) and into the pGBKT7 vector to generate pGBK-Baits (BD-OsbHLH156 and BD-OsIRO2). Yeast two-hybrid assays were performed as described previously with modifications (Ying *et al.*, 2017). The plasmids with different

combinations of pGAD-Preys and pGBK-Baits were transformed into *Saccharomyces cerevisiae* AH109 (WEIDI, Shanghai, China) according to the manufacturer's instructions, and grown on synthetically defined (SD) medium lacking Leu and Trp (SD/–Leu/–Trp). The positive transformants that grew on SD/–Leu/–Trp were spotted onto minimal media quadruple dropout (QDO; SD/–Leu/–Trp/–His/–Ade) plates and grown for 4–5 d. Ten millimole 3-amino-1, 2, 4-triazole (3-AT) was added to the QDO to inhibit self-activation. The empty vectors pGADT7-Rec (AD) and pGBKT7 (BD) were used as negative controls.

Transcriptional activation assay

Transcriptional activation assays were performed as described previously with modifications (Yuan *et al.*, 2008). For yeast assays, the CDS of the β-glucuronidase (*GUS*) gene was inserted into pAG426 at the *Hin*dIII and *Sac*I sites to generate a *GUS* expression vector in yeast, named pAG426-GUS. The promoters of *OsIRT1*, *OsYSL15*, *OsNRAMP6*, *OsCOPT1/7*, *OsZIP5/9/10*, *OsHMA2*, *OsNAS1*, *OsNAS2*, *OsNAAT1*, *OsTOM1*, and *OsACTIN1* were cloned into the pAG426-*GUS* vector, generating 13 vectors, namely P_{OsIRT1}-GUS, $P_{OsYSL15}$-GUS, $P_{OsNRAMP6}$-GUS, $P_{OsCOPT1/7}$-GUS, $P_{OsZIP5/9/10}$-GUS, P_{OsNAS1}-GUS, P_{OsNAS2}-GUS, $P_{OsNAAT1}$-GUS, P_{OsTOM1}-GUS, and $P_{OsACINT1}$-GUS. The P_{gene}-GUS plasmids were transformed together with one of the following construct combinations: AD-OsbHLH156 and BD-OsIRO2 or BD-OsbHLH156 and AD-OsIRO2 into *Saccharomyces cerevisiae* AH109 (WEIDI). The yeast cells were grown on SD/–Leu/–Trp/–Ura for 4–5 d. After which positive transformants were suspended using sterile deionized water and adjusted to an OD_{600} of 1.0. These yeast suspensions (20 μl) were placed into tubes and centrifuged at 5000 rpm for 2 min. The liquid supernatant was removed, and the yeast cells were incubated with GUS staining buffer {10 mM Na_2EDTA, 1 mM $K_3[Fe(CN_6)]$, 1 mM $K_4[Fe(CN_6)]$}, 100 mM sodium phosphate buffer, pH 7.0, 0.5% (v/v) Triton X-100, 20% (v/v) methanol, and 0.5 mg ml^{-1} 5-bromo-4-chloro-3-indolyl- D-glucuronic acid (X-gluc) at 37 °C overnight.

For the luciferase (LUC) assay, CDS of *OsbHLH156* and *OsIRO2* were amplified from cDNA with gene-specific primers and cloned into the pCAMBIA1300 vector, driven by the *Cauliflower mosaic virus* (CaMV) 35S promoter. The promoters of target genes were amplified from Nipponbare genomic DNA and fused within the luciferase reporter vector. *Agrobacterium tumefaciens* EHA105 harbouring different combinations of P_{gene}-*LUC*, *35S:OsbHLH156* and *35S:OsIRO2* were mixed to infiltrate tobacco (*Nicotiana benthamiana*) leaf epidermal cells. After 3 d of infiltration, the leaves were detached and sprayed with 0.2 mg ml^{-1} potassium luciferin [Yeasen Biotechnology (Shanghai) Co., Ltd., Shanghai, China] and incubated in the dark for 5 min. Luminescence was imaged using the NightShade LB 985 system (Berthold, Germany) and quantitated using IndiGO software (Hao *et al.*, 2022).

Nuclear protein extraction and western blot analysis

Fresh root samples were harvested from the WT and transgenic plants (*OsIRO2-mCherry*/WT and *OsIRO2-mCherry*/*osbhlh156*) grown under Fe-sufficient and deficient conditions hydroponically. Nuclear proteins were extracted according to a previously described protocol (Saleh *et al.*, 2008). The root tissues (about 4 g of each sample) from transgenic plants (*OsIRO2-mCherry*/WT and *OsIRO2-mCherry*/*osbhlh156*) were collected, and ground to a fine powder in pre-chilled mortars. Twenty microlitres of cold nuclei isolation buffer containing 0.25 M sucrose, 15 mM piperazine-*N*, *N*'-bis (2-ethanesulfonic acid) (PIPES, pH 6.8), 5 mM $MgCl_2$, 60 mM KCl, 15 mM NaCl, 1 mM $CaCl_2$, 0.9% Triton X-100, 1 mM phenylmethylsulfonyl fluoride (PMSF), and 1× protease inhibitor cocktail (Sigma-Aldrich, MO, USA) was used to resuspend each sample. The sample were then vortexed briefly and kept on ice, these steps were alternated for 20 min. The homogenized slurry was filtered through four layers of Miracloth and the filtrate centrifuged at 11 000 g for 20 min. The supernatant was discarded and the pellet resuspended using nuclei isolation buffer followed by boiling with protein loading buffer to extract the nuclear protein. Protein samples were loaded on 12% SDS-PAGE gels, and transferred to polyvinylidene fluoride membranes. The target proteins were detected by rabbit polyclonal anti-mCherry (1:5000; Abcam, England) and anti-Histone H3 (1:5000; Abcam, England).

Results

OsbHLH156 and OsIRO2 are involved in Mn, Cu, and Zn accumulation under Fe deficiency

A previous study has shown OsbHLH156 regulates Strategy II iron acquisition through localizing IRO2 to the nucleus in rice (Wang *et al.*, 2020). To further investigate the effects of *OsbHLH156* and *OsIRO2* on Fe homeostasis, *osbhlh156* and *osiro2* mutants were generated using CRISPR/Cas9. Two *osbhlh156* mutant lines and two *osiro2* mutant lines were characterized (*osbhlh156*-1 was described in Wang *et al.*, 2020; Supplementary Fig. S1). As expected, both *osbhlh156* and *osiro2* mutants showed growth defects, leaf chlorosis, and reduced shoot Fe concentration when grown in upland soil where only Fe(III) was available (Supplementary Fig. S2).

To test the effect of the OsbHLH156–OsIRO2 TF complex on the uptake and transport of other divalent metals, shoot tissues of the WT and the *osbhlh156* and *osiro2* mutants were collected for the determination of element concentrations by inductively coupled plasma mass spectrometry (ICP-MS). While the Fe-deficient condition led to significant increases of Mn, Cu, and Zn concentrations in WT shoots, these increases were inhibited in the *osbhlh156* and *osiro2* mutants. Compared to the WT, shoot Mn, Cu, and Zn concentrations in the two mutants showed similar degrees of decline, with Mn decreasing by 37.9%, Cu by 35.8%, and Zn by 23.6% (Fig. 1). Under the Fe-sufficient condition, only the Mn concentration slightly decreased in the *osbhlh156* and *osiro2* mutants, and no effect could be observed on Cu and Zn concentrations (Fig. 1). These results demonstrated that the OsbHLH156–IRO2 TF complex is critical for increased Mn, Cu, and Zn accumulation under Fe deficiency.

The OsbHLH156–OsIRO2 TF complex regulates expression of genes encoding Mn, Cu, and Zn transporters

To determine genes regulated by the OsbHLH156–OsIRO2 TF complex, RNA sequencing (RNA-seq) analysis of the shoots and roots from the WT and *osbhlh156* and *iro2* mutants was performed. Under Fe-replete conditions, although shoot Fe concentrations in the *osbhlh156* and *osiro2* mutants were lower than the WT, no other obvious phenotypic changes were observed. Comparative transcriptome analysis revealed 91 and 32 DEGs in the comparisons of the *osbhlh156* and *osiro2*

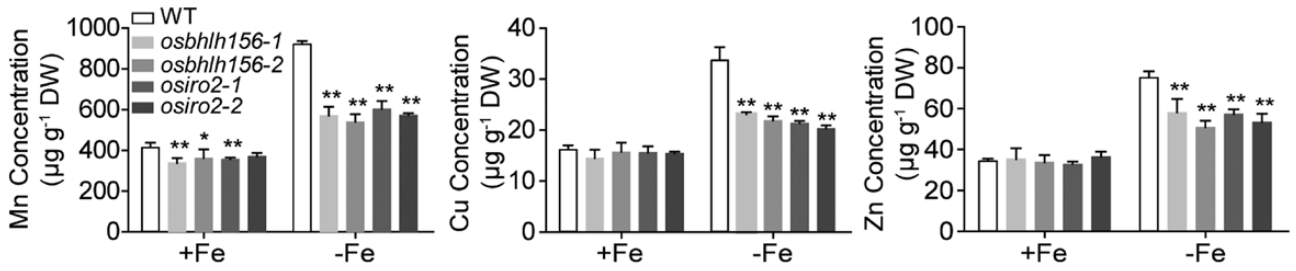

Fig. 1. OsbHLH156 and OsIRO2 regulate uptake and translocation of Mn, Cu, and Zn. The plants were grown in hydroponic culture with or without Fe. The shoots were collected from WT, *osbhlh156*, and *osiro2* plants grown in Fe-sufficient or Fe-deficient conditions for 10 d. Three independent measurements in three independent plants were performed for elements analysis. The concentrations of Mn, Cu, and Zn were determined by ICP-MS. Data represent means ±SD, n=3; *, P<0.05; **, P<0.01 (Student's t-test).

mutants versus the WT, respectively (Supplementary Fig. S3; Supplementary Table S2). Under Fe-depleted conditions, *osbhlh156* and *osiro2* mutants showed growth defects, leaf chlorosis, reduced SPAD value, and lower shoot Fe concentration in comparison to the WT (Fig. 2A, B). The number of DEGs is almost 10–20 times higher than those under Fe-replete conditions. Moreover, 85 genes induced by Fe deficiency in the WT were significantly down-regulated in both the *osbhlh156* and *osiro2* mutants, and 117 genes suppressed by Fe deficiency in the WT were up-regulated in the *osbhlh156* and *osiro2* mutants (Fig. 2C, D; Supplementary Table S3). Overall, genes involved in Strategy II Fe acquisition, including MA synthesis, the S-adenosylmethionine cycle, and Fe transport, no longer responded to Fe deficiency in the *osbhlh156* or *osiro2* mutants (Supplementary Table S4). Gene Ontology (GO) and Kyoto Encyclopedia of Genes and Genomes (KEGG) analysis showed that 288 (the sum of red numbers in Fig. 2C) Fe-deficiency DEGs meanwhile potentially regulated by bHLH156 or IRO2 were enriched predominantly in genetic information processing, ribosome biogenesis, DNA replication, hierarchies, signalling and cellular processes (Fig. 2E; Supplementary Tables S5, S6), implying that there must be other downstream pathways regulated by these two TFs. To determine the effect of OsbHLH156 and OsIRO2 on accumulation of Mn, Cu, and Zn, the expression profiles of genes encoding Mn, Cu, and Zn transporters were extracted from the RNA-seq data and summarized in heatmaps (Fig. 3A).

Among the Mn transporter genes, two Natural Resistance-Associated Macrophage Protein (NRAMP) family members were significantly suppressed in the *osbhlh156* and *osiro2* mutants. *OsNRAMP5* encodes a Mn transporter that is required for Mn uptake and shows polar localization at the distal side of both exodermis and endodermis cells (Sasaki *et al.*, 2012), that was suppressed in the root of the *osbhlh156* and *osiro2* mutants (Fig. 3A). *OsNRAMP6*, responsible for Mn and Fe transport (Peris-Peris *et al.*, 2017), was suppressed in the shoots of the mutants (Fig. 3A). OsMTP9 (Metal Tolerance Protein 9) belongs to the cation diffusion facilitator family, localizes to the proximal side of exodermis and endodermis cells (the opposite of OsNRAMP5), and plays an important role in Mn translocation to the root stele (Ueno *et al.*, 2015). In this study, expression of *OsMTP9* was significantly inhibited in both *osbhlh156* and *osiro2* roots compared with the WT under Fe deficiency. Two Yellow Stripe-Like (YSL) genes, encoding Mn(II)-nicotianamine complex transporters, showed contrary expression patterns. *OsYSL2*, required for the long-distance transport of Fe and Mn in rice (Ishimaru *et al.*, 2010), was induced in both *osbhlh156* and *osiro2* under Fe deficiency, whereas *OsYSL6*, required for the detoxification of excess Mn in rice (Sasaki *et al.*, 2011), was suppressed in both *osbhlh156* and *osiro2* (Fig. 3A).

At least three Cu transporters in rice have been reported, including *OsHMA5*, *OsYSL16*, and *COPT7*. OsHMA5 is localized in the root pericycle cells and the xylem region of diffuse vascular bundles in node I and is required for Cu loading into the xylem of the roots (Deng *et al.*, 2013). Another Cu transporter, OsYSL16, is mainly expressed in the phloem of nodes and vascular tissues of leaves. Knocking out of *OsYSL16* resulted in 22% and 20% lower Cu concentration in roots and shoots, respectively (Zheng *et al.*, 2012). OsCOPT7 mediates high-affinity Cu uptake in the yeast mutant (Yuan *et al.*, 2011). The expression of *OsHMA5*, *OsYSL16*, and *OsCOPT7* in Fe-depleted medium were all significantly suppressed in roots of both *osbhlh156* and *osiro2* (Fig. 3A).

For the Zn transporter genes, 5 ZIP (Zrt, Irt-like protein) family members were suppressed in both the *osbhlh156* and the *osiro2* mutants. *OsZIP4* encodes a Zn transporter, localizes to root apical cells, and is responsible for Zn translocation (Ishimaru *et al.*, 2005, 2007). Both *OsZIP5* and *OsZIP9* are expressed in the root epidermis and function synergistically in Zn uptake (Tan *et al.*, 2020). *OsZIP7* is required for Zn homeostasis, and the distribution of Zn in *oszip7* is maladjusted, accumulating in the roots and decreasing in the shoots (Gindri *et al.*, 2020). *OsZIP10* encodes a plasma membrane-localized Zn transporter and the transcript of the *OsZIP10* gene is associated with Zn content in rice grains (Maurya *et al.*, 2018). *OsHMA2* is mainly expressed in the mature zone of the roots and functions as a facilitator of Zn translocation through the phloem to the developing tissues (Yamaji *et al.*, 2013). In this study, the expression level was significantly lower in Fe-deficient *osbhlh156* and *osiro2* mutant roots than in the WT (Fig. 3A).

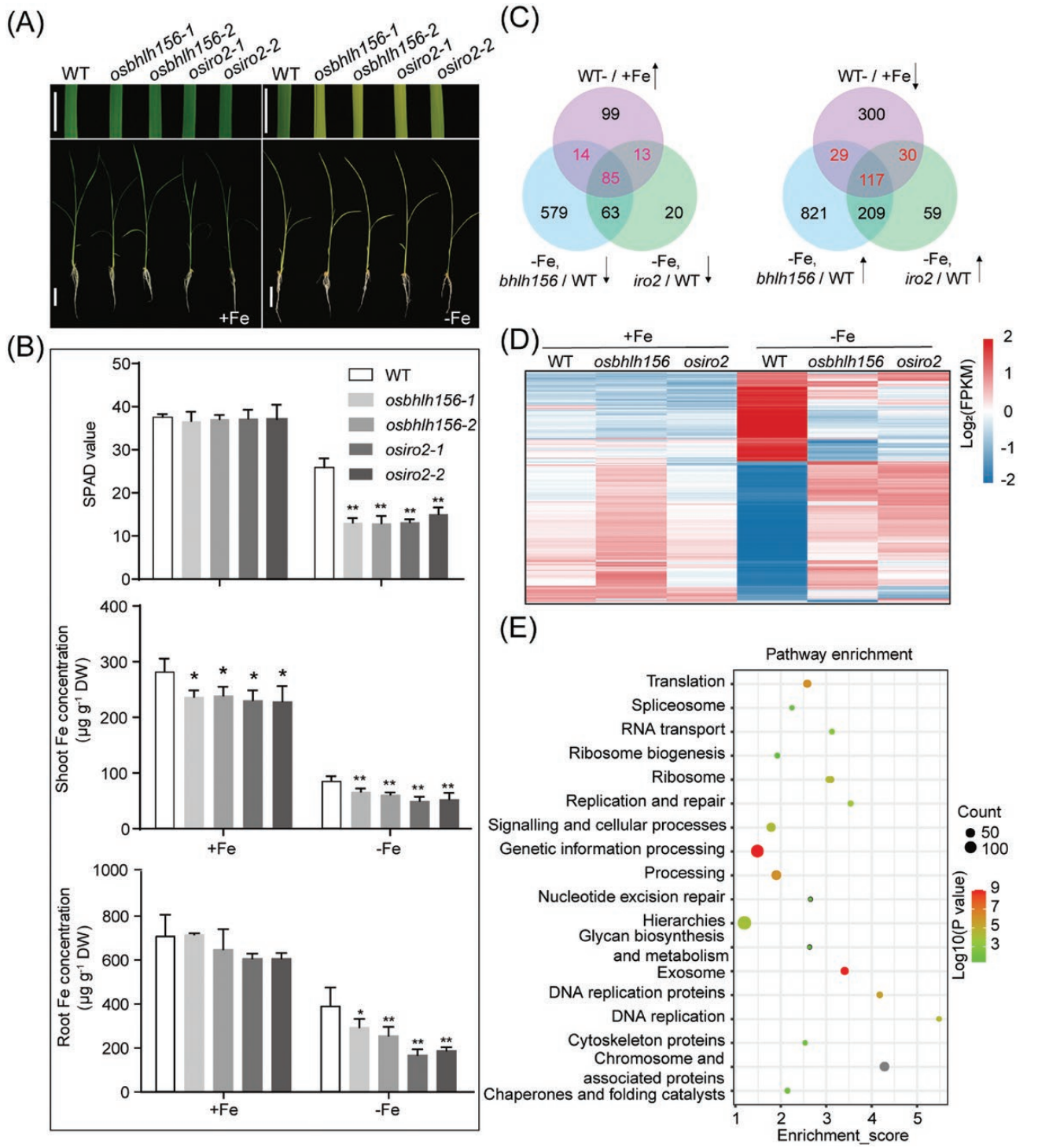

Fig. 2. Characterization of *osbhlh156* and *osiro2* mutant lines. (A) Ten-day-old *osbhlh156* and *osiro2* seedlings grown under Fe-sufficient and Fe-deficient conditions. The plants were grown in hydroponic culture with or without Fe. Upper bars=1 cm; lower bars=3 cm. (B) SPAD value and Fe concentration. The shoots and roots were collected from WT, *osbhlh156*, and *osiro2* plants grown in Fe-sufficient or Fe-deficient conditions for 10 d. Fe concentration was detected by ICP-MS. Data represent means ±SD, n=3; *, P<0.05; **, P<0.01 (Student's t-test). (C) Venn diagrams of the number of DEGs. (D) Heatmap of 245 genes (14 + 85 + 29 + 117) downstream of *OsbHLH156* and of 245 genes (13 + 85 + 30 + 117) downstream of *OsIRO2* in root. (E) KEGG enriched pathways of DEGs between WT and mutants (*osbhlh156* and *osiro2*). The colour and size of the dot represents the P value and the number of DEGs mapped to the reference pathways, respectively. Eight independent measurements were performed for SPAD. Three independent measurements in three independent plants were performed for elements and transcriptome analysis.

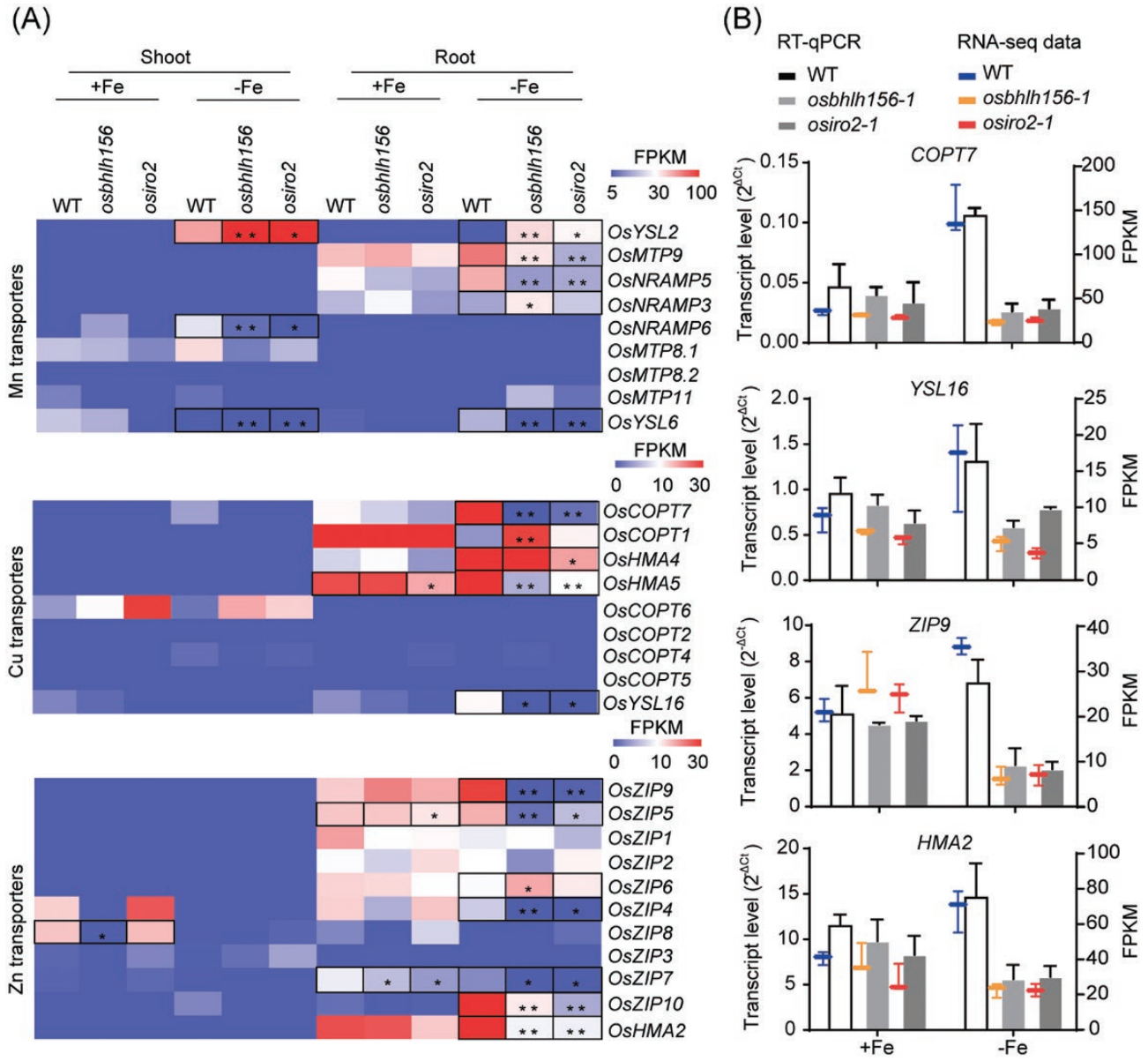

Fig. 3. Expression pattern of the indicated Mn, Cu, and Zn transporter genes in WT, *osbhlh156*, and *osiro2* plants. (A) RNA-seq data. Colours represent gene expression levels as FPKM. Significance of each difference compared with WT is indicated by asterisks. *n*=3; *, *P*<0.05; **, *P*<0.01 (Student's *t*-test). (B) RT–qPCR validation. Four transporter genes were chosen to perform RT–qPCR analysis using root tissues. The relative expression level from the RT-PCR is presented on the left axis, the right shows the FPKM value from RNA-seq data. *OsACTIN1* was used as a reference gene. The data represents the means ±SD determined using three biological repeats, each biological repeat was pooled from three independent plants.

RT–qPCR analysis of *OsCOPT7*, *OsYSL16*, *OsZIP9*, and *OsHMA2* was performed to verify the expression level from the RNA-seq data. The expression of these genes was all significantly suppressed in both the *osbhlh156* and *osiro2* mutants under Fe deficiency, which showed a consistent trend with the RNA-seq data (Fig. 3B). *OsACTIN1* was used as an internal control, and its expression was consistent under different growth conditions when normalized by UBQ (Supplementary Fig. S4).

The OsbHLH156–OsIRO2 TF complex activates the promoters of divalent metal transporter genes

Previously, an *in vitro* experiment based on tobacco agroinfiltration showed that OsbHLH156 facilitates nuclear localization of OsIRO2 under Fe-deficient conditions (Wang *et al.*, 2020). Here, *in vivo* verification was conducted using stable transgenic rice plants. The genomic DNA sequence of *OsIRO2* was fused to *mCherry* and expressed in WT or

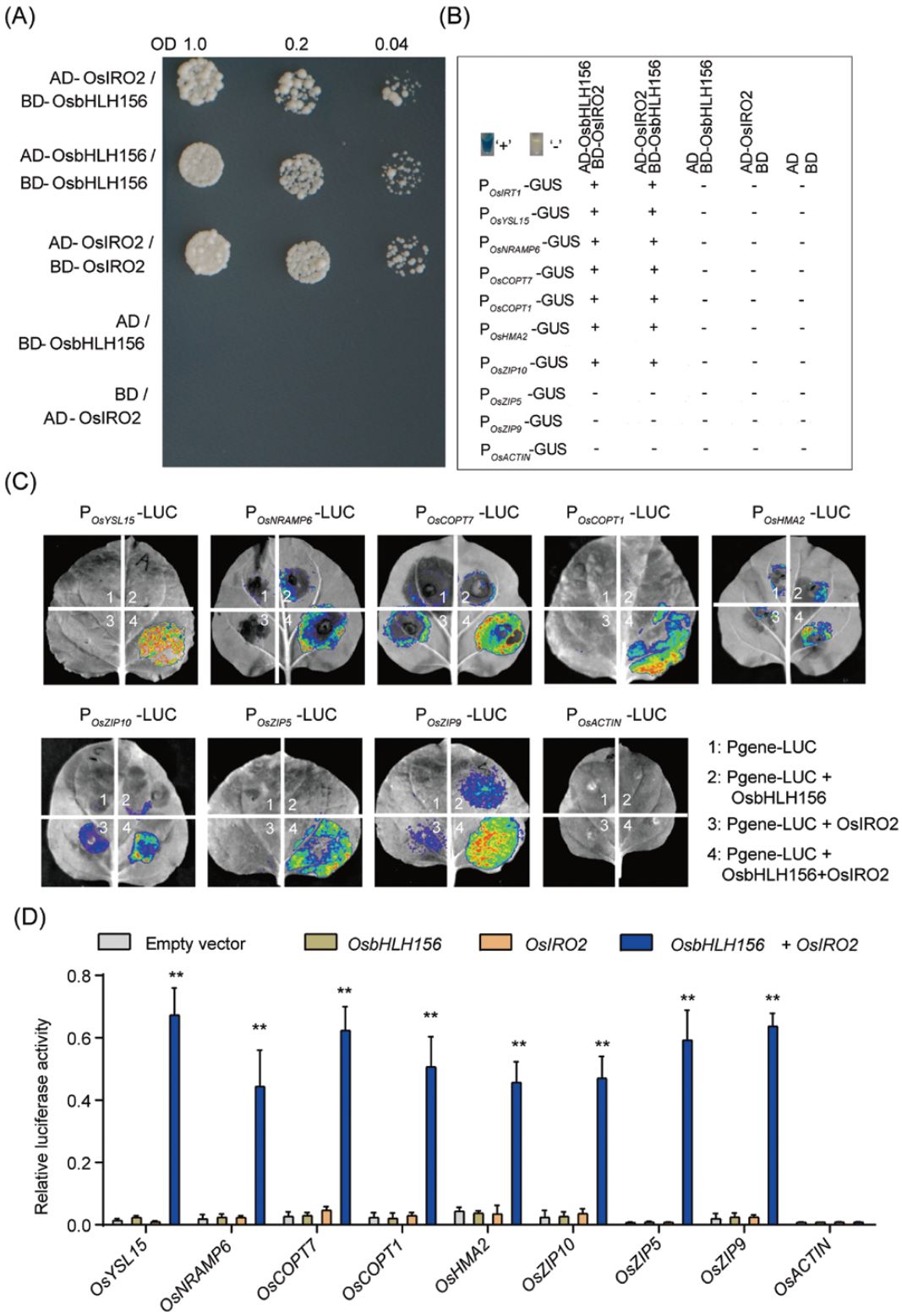

Fig. 4. The OsbHLH156–OsIRO2 TF complex is required for activating the Fe, Mn, Cu, and Zn transporter genes. (A) Yeast two-hybrid assay. OsbHLH156 and OsIRO2 were fused with the GAL4 activation domain (AD) or the GAL4 DNA binding domain (BD). The different combinations of expression vectors were then transferred into yeast cells (*Saccharomyces cerevisiae* AH109). The different yeast strains were plated on selection medium QDO with 10 mM 3-amino-1, 2, 4-triazole (3-AT). The empty vectors AD and BD were used as negative controls. (B) Transcriptional activation assay. The *GUS* gene was fused with a native promoter of one of the target genes and co-expressed with *OsbHLH156* or *OsIRO2*, or both, in yeast. The yeast cells were grown on selection medium (–Trp, –Leu, –Ura), and stained using GUS buffer. The blue colour (+) indicated that the reporter gene

GUS was transcribed. (C) Expression of luciferase in *Agrobacterium*-infiltrated tobacco leaves. Each of the eight promoter-luciferase fusions (P_{gene}-LUC) was expressed in tobacco leaves with no recombinant transcription factor (1), with either OsbHLH156 (2) or OsIRO2 (3), or with both OsbHLH156 and OsIRO2 (4). The promoter of *OsACTIN1* was used as a negative control (final panel). (D) Luciferase activity. Relative luciferase activity was calculated compared with the vector control. Three independent experiments were performed. Data represent means ±SD (n=3); **, P<0.01 (Student's t-test).

osbhlh156 mutant rice. While the OsIRO2 protein accumulated in the nucleus of Fe-deficient WT plants, OsIRO2 accumulation was largely absent in the nucleus of the *osbhlh156* mutant (Supplementary Fig. S5A). For further confirmation of the tissue and subcellular localization of OsIRO2, *in situ* immunostaining was performed using rice roots. The mCherry antibody signals from *pOsIRO2-gOsIRO2-mCherry/osbhlh156* were observed mainly in the cytoplasm, and just a small fraction of the signal was in the nucleus. When OsIRO2-mCherry was expressed in WT background, most of the mCherry antibody signals were located in the nucleus (Supplementary Fig. S5B). The above results confirmed that OsbHLH156 is essential for nuclear localization of IRO2 *in vivo*. The temporal expression of *OsbHLH156* and *OsIRO2* in response to Fe deficiency showed that *OsbHLH156* and *OsIRO2* synchronously respond to Fe deficiency in rice roots (Supplementary Fig. S6). Thus, Fe deficiency activates the OsbHLH156–OsIRO2 TF complex, which in turn actives further Fe deficiency responses.

In order to study whether the OsbHLH156–OsIRO2 TF complex can activate the transcription of Mn, Cu, and Zn transporter genes, we performed transcriptional activation assays in yeast cells. First, a yeast two-hybrid assay confirmed that OsbHLH156 could form a complex with OsIRO2 in yeast cells (Fig. 4A). The potentially downstream divalent metal transporters, including *OsIRT1*, *OsYSL15*, *OsNRAMP6*, *OsHMA2*, *OsZIP5/9/10*, and *OsCOPT1/7*, were selected for transcriptional activation assays as previously described (Yuan *et al.*, 2008). The constructs using promoters of these potential target genes to drive the *GUS* reporter gene were expressed in yeast cells together with the constructs containing either OsbHLH156 or OsIRO2, or both. While neither OsbHLH156 nor OsIRO2 alone could activate the expression of the reporter gene (Fig. 4B, third and fourth columns), OsbHLH156 and OsIRO2 together could activate the promoters of *OsIRT1*, *OsYSL15*, *OsNRAMP6*, *OsHMA2*, *OsCOPT1/7*, and *OsZIP10*, but not of *OsZIP5* and *OsZIP9* (Fig. 4B; Supplementary Fig. S7). Luciferase reporter assays showed that all eight tested candidate genes, i.e. *OsYSL15*, *OsNRAMP6*, *OsHMA2*, *OsCOPT1/7*, and *OsZIP5/9/10*, were activated by the OsbHLH156–OsIRO2 TF complex, but the single TFs could not do so (Fig. 4C, D). The inconsistent results between the yeast one-hybrid and luciferase assays on *OsZIP5/9* implied that there might be other partner(s) interacting with the OsbHLH156–OsIRO2 TF complex for transcription of these two genes. Taken together, the direct transcriptional activation of these metal transporter genes is one of the ways that the OsbHLH156–OsIRO2 TF complex regulates Mn, Cu, and Zn homeostasis.

The OsbHLH156–OsIRO2 TF complex affects divalent metal homeostasis via the NA and DMA pathways

Previous studies have proved that NA and DMA are very important chelators for Fe, Mn, Cu, and Zn during their uptake and translocation (Pich and Scholz, 1996; Takahashi *et al.*, 2003; Kobayashi and Nishizawa, 2012; Nishiyama *et al.*, 2012; Rai *et al.*, 2021). RNA-seq and RT–qPCR analysis showed that genes involved in the NA and DMA synthesis pathways, including *OsNAS1*, *OsNAS2*, *OsNAAT1*, and *OsTOM1*, were severely down-regulated in the *osbhlh156* and *osiro2* mutants under Fe deficiency (Fig. 5A; Supplementary Table S4). To examine whether NA and DMA synthesis were altered in these mutants, NA concentration in the root and DMA concentration in root exudate of rice plants grown under Fe deficiency were determined by LC-MS. The results showed that the NA content in *osbhlh156* and *osiro2* mutant roots was decreased by more than 50% compared to WT, whereas the DMA exudate was almost completely abolished in these mutants (Fig. 5B).

Yeast one-hybrid and luciferase reporter assays were used to test whether genes involved in NA and DMA synthesis are regulated by the OsbHLH156–OsIRO2 TF complex. As shown in Fig. 5C, E, the promoters of *OsNAS1*, *OsNAS2*, and *OsNAAT1*, but not *OsTOM1*, could be activated by the OsbHLH156–OsIRO2 TF complex. The luciferase reporter assay also showed that *OsNAS1*, *OsNAS2*, and *OsNAAT1* were activated by the TF complex (Fig. 5D, E). These results support the idea that the OsbHLH156-OsIRO2 TF complex regulates Mn, Cu, and Zn homeostasis through promoting the synthesis of divalent metal chelators.

Roles of the OsbHLH156–OsIRO2 TF complex in Fe and Cu interaction

The involvement of the OsbHLH156–OsIRO2 TF complex in the regulation of Mn, Cu, and Zn accumulation under Fe deficiency may be attributed to the direct responses of *OsbHLH156* and *OsIRO2* to Mn, Cu, or Zn deficiency. To test this hypothesis, the expression levels of *OsbHLH156* and *OsIRO2* were detected under different nutrient deficient conditions in rice roots. While both TF genes were induced by Fe deficiency as previously reported (Wang *et al.*, 2020), the transcripts of *OsbHLH156* and *OsIRO2* were induced by Mn deficiency and Cu deficiency, respectively (Fig. 6A, B). The SPAD

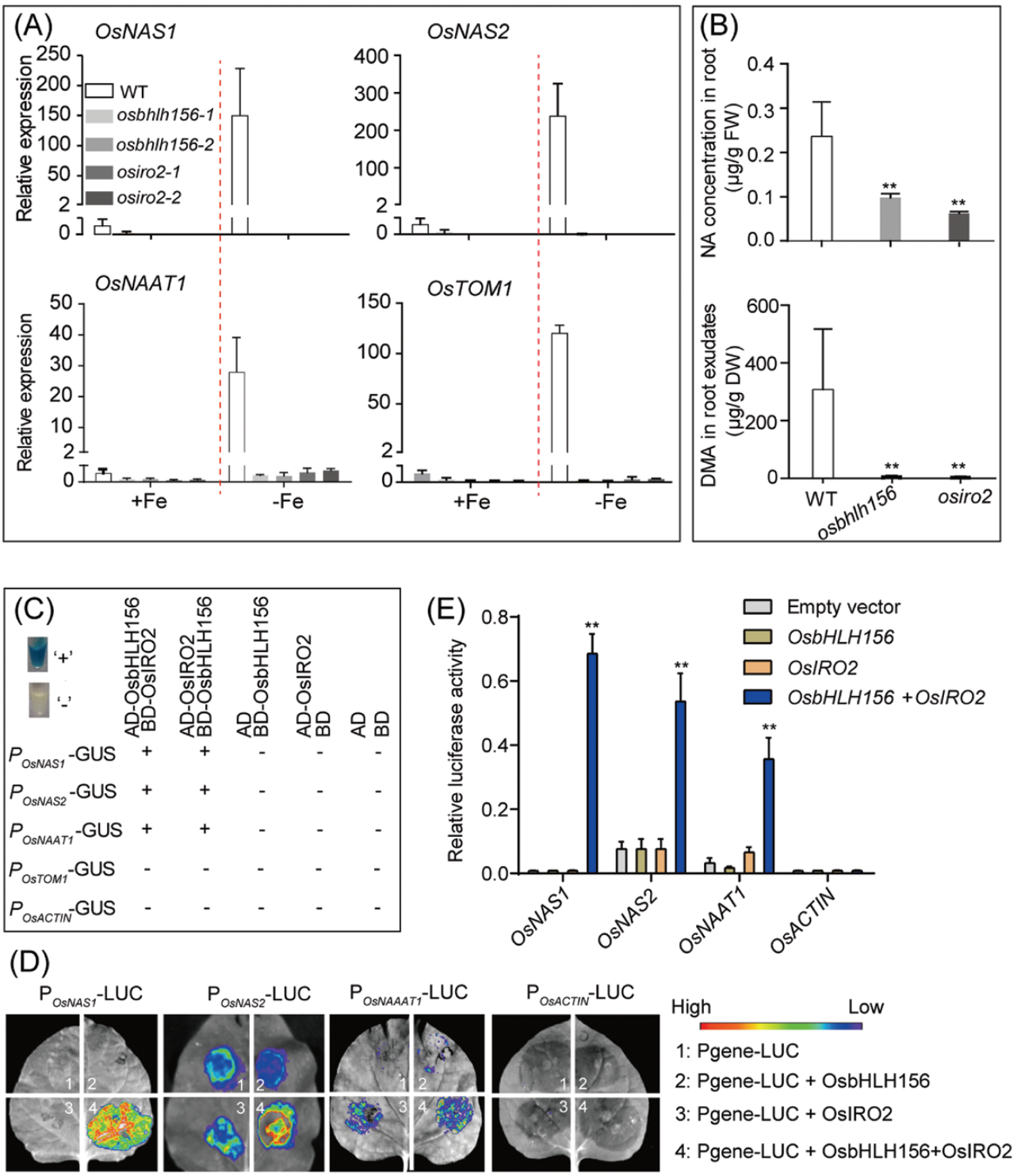

Fig. 5. NA and DMA biosynthesis are directly regulated by the OsbHLH156–OsIRO2 TF complex. (A) Expression of genes involved in NA and DMA synthesis and DMA secretion. The plants were grown in Fe-sufficient or Fe-deficient solutions for 10 d. *OsACTIN1* was used as the internal control to normalize the samples. (B) NA and secreted DMA content. Amount of NA in the root and DMA secreted from root were detected from WT, *osbhlh156*, and *osiro2* plants under Fe deficiency. (C) Transcriptional activation assay. The *GUS* gene was fused with a native promoter of one of the four target genes and co-expressed with *OsbHLH156* or *OsIRO2*, or both, in yeast. The promoter of *OsACTIN1* was used as a negative control. (D) Expression of luciferase in *Agrobacterium*-infiltrated tobacco leaves. Each of four promoter-luciferase fusions (P_{gene}-LUC) was expressed in tobacco leaves with no recombinant transcription factor (1), with either OsbHLH156 (2) or OsIRO2 (3), or with both OsbHLH156 and OsIRO2 (4). The promoter of *OsACTIN1* was used as a negative control (final panel). (E) Luciferase activity. Relative luciferase activity was calculated compared with the vector control. Three independent experiments were performed. Data represent means ±SD (n=3); **, P<0.01 (Student's t-test).

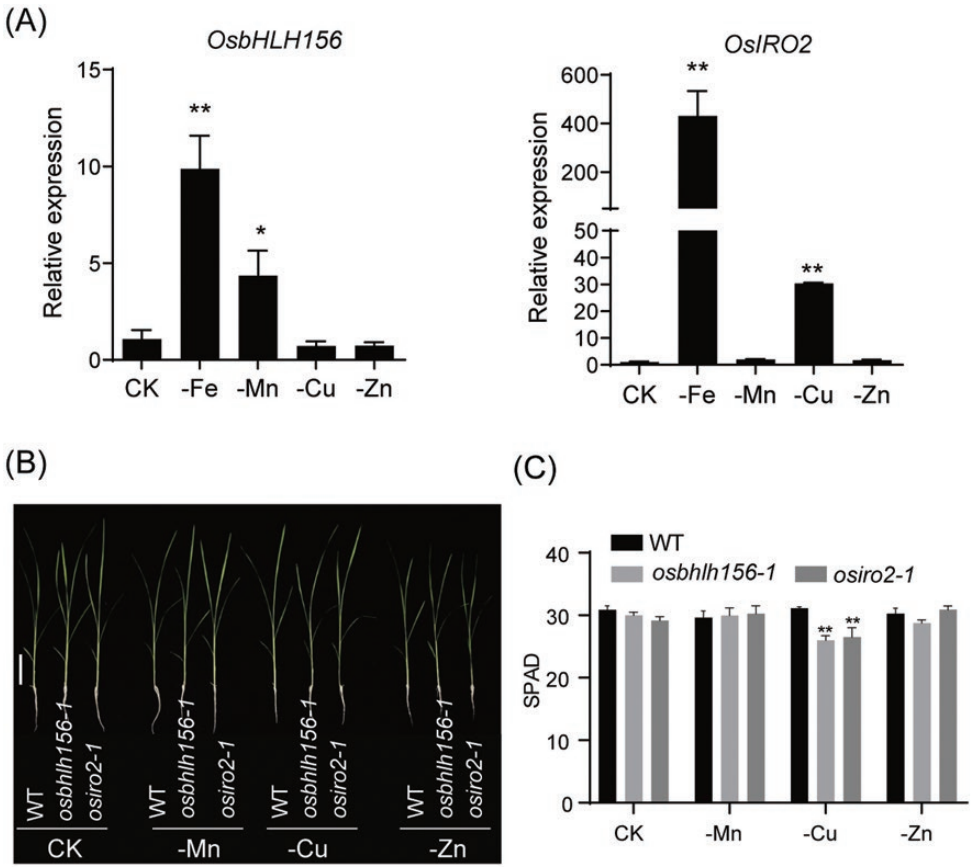

Fig. 6. Phenotypes of rice seedlings grown under different nutrient deficient conditions. (A) Relative expression of *OsbHLH156* and *OsIRO2* under different nutrient deficient conditions. Rice roots of WT Nipponbare plants were collected for RNA extraction and quantitative RT-PCR. Three independent measurements in three independent plants were performed for RT-PCR. *OsACTIN1* was used as the internal control to normalize the samples. Data represent means ±SD, n=3; *, P<0.05; **, P<0.01 (Student's t-test). (B) Sixteen-day-old *osbhlh156* and *osiro2* seedlings. Bar=6 cm. (C) SPAD value. Data represent means ±SD, n=8; **, P<0.01 (Student's t-test). Eight independent measurements were performed for SPAD.

value of the *osbhlh156* and *osiro2* mutants were significantly lower than that of the WT under Cu deficiency, but not under Mn- or Zn-deficient conditions (Fig. 6C). No difference in shoot height, root length, or shoot and root biomass could be observed between the WT and the mutants under different nutrient deficient conditions (Supplementary Fig. S8). These results implied that OsbHLH156 and OsIRO2 might be involved in Fe and Cu crosstalk.

To further investigate whether *OsbHLH156* and *OsIRO2* participate in crosstalk between Fe and Cu, the *osbhlh156* and *osiro2* mutants were grown under four nutrient conditions, including full strength Fe and Cu (CK), full strength Cu but no Fe (–Fe), full strength Fe but no Cu (–Cu) and without both Fe and Cu (–Fe–Cu). As shown in Fig. 7A, B, the *osbhlh156* and *osiro2* mutants showed lower SPAD values than the WT when grown in the –Fe, –Cu, and –Fe–Cu conditions. The shoot Fe concentrations of the *osbhlh156* and *osiro2* mutants were significantly lower than those of the WT under all four conditions, while the root Fe concentrations of these mutants were reduced only in the –Fe and –Cu conditions (Fig. 7C, D). Cu concentrations in mutants decreased only in shoots under Fe deficiency and in roots of the CK and –Fe treatments (Fig. 7E, F).

Although the Fe concentrations in the shoots of the *osbhlh156* and *osiro2* mutants were significantly lower than in the WT under the Cu-deficient condition, both mutants showed similar large decreases in Fe content in CK treatment (Fig. 7C). It is worth noting that under the control conditions, there was no significant difference between the SPAD value of the mutants and the WT, but the SPAD value did differ significantly in the absence of Cu (Fig. 7B). We speculated that under CK conditions, sufficient Cu supply may compensate, at least partially, for the function of Fe in chlorophyll synthesis and alleviate the Fe-deficiency phenotype. To test this hypothesis, rice seedlings were grown without Fe but with three times the amount of Cu (++Cu). As shown in Supplementary Fig. S8, increase of Cu supply alleviated leaf chlorosis and reduced accumulation of reactive oxygen species caused by Fe deficiency. Thus, in response to Fe deficient stress, the activated OsbHLH156–OsIRO2 TF complex not only induces

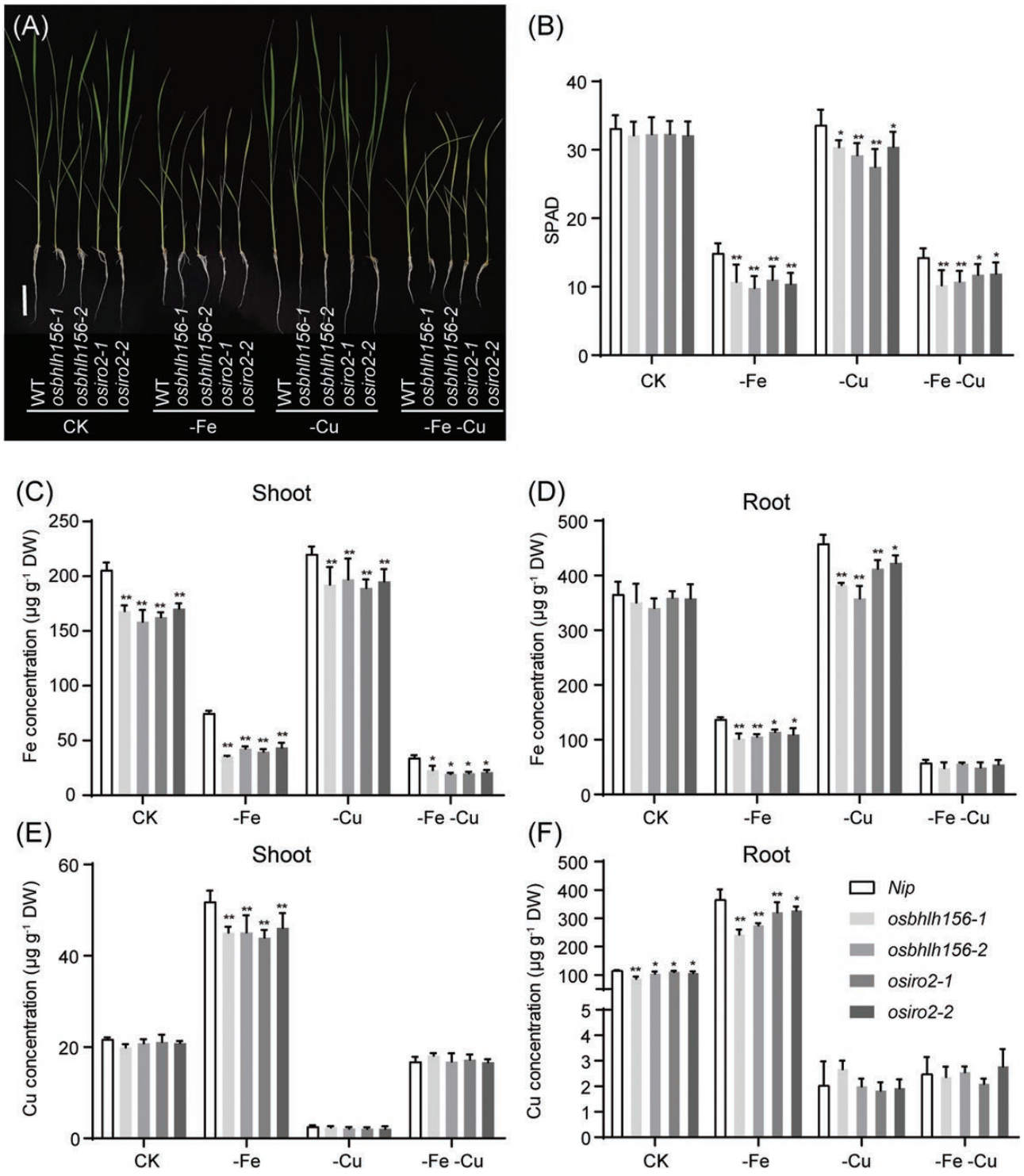

Fig. 7. Phenotypes of *osbhlh156* and *osiro2* mutant lines grown under different nutrient regimes for 3 weeks. (A) Growth performance of *osbhlh156* and *osiro2* mutants grown under four different treatments. Bar=5 cm. (B) SPAD values. (C) Fe concentration in shoots. (D) Fe concentration in roots. (E) Cu concentration in shoots. (F) Cu concentration in roots. Data represent means ±SD (SPAD, n=8; element concentration, n=4); *, P<0.05; **, P<0.01 (Student's t-test). Eight independent measurements were performed for SPAD. Four independent measurements in three independent plants were performed for element analysis.

Fe uptake, but also Cu uptake, which helps plants cope with Fe-deficiency stress.

Discussion

Fe-deficiency stress in plants can markedly induce both the accumulation of Mn, Cu, and Zn, and the expression level of genes encoding the transporters of these micronutrients (Welch *et al.*, 1993; Cohen *et al.*, 1998; Vert *et al.*, 2002). The most common explanation for this is the low selectivity of some universal metal transporters like IRT1, NRAMPs, which can transport Mn, Cu, and Zn (Grotz and Guerinot, 2006). In this study, we explored the role of the Fe-deficiency induced OsbHLH156–OsIRO2 TF complex in Mn, Cu, and Zn homeostasis. We found that the increased accumulation of Mn, Cu, and Zn concentrations under Fe deficiency was largely dependent on the OsbHLH156–OsIRO2 TF complex. The OsbHLH156–OsIRO2 TF complex not only activates the transcription of metal transporter genes but also the synthesis of NA and DMA, which are important metal chelators for the uptake and transport of Fe, Mn, Cu, and Zn. Lack of either TF (OsbHLH156 or OsIRO2) in the complex significantly reduced the Mn, Cu, and Zn accumulation (Fig. 1).

The OsbHLH156–OsIRO2 TF complex is effective under upland conditions

Rice possesses both the Fe(II) uptake mechanism (Strategy I-like) and the Fe(III) uptake mechanism (Strategy II) (Ishimaru *et al.*, 2006; Cheng *et al.*, 2007). Given the fact that the OsbHLH156–OsIRO2 TF complex functions under upland conditions when Fe(III) is the major form of Fe source (Liang *et al.*, 2020; Wang *et al.*, 2020), the role of the TF complex on Mn, Cu, and Zn homeostasis should mainly occur under upland conditions. In contrast, the low-selective metal transporters such as IRT- and NRAMP-type transporters should be effective mostly in flooding conditions. Future studies using both flooding and upland treatments could further elucidate the relative importance of the mechanisms involving in the crosstalk of Fe with Mn, Cu, and Zn in rice.

The low-selectivity of the direct target transporters of the OsbHLH156–OsIRO2 TF complex

Functions of the micronutrients Mn, Cu, and Zn are tightly linked for vital metabolism. Their homeostasis must be tightly regulated to maintain their optimal concentration for biological functions to avoid oxidative injuries due to their accumulation (Grotz and Guerinot, 2006). As a Strategy I plant species, *Arabidopsis* uses mainly IRT- and NRAMP-type transporters to uptake Fe(II) reduced by ferric reductase oxidase (FRO). Adapted to the flooding condition, rice is an exception of Strategy II plant species that possesses a Strategy I-like Fe(II) uptake system using Fe(II) transporters similar to their *Arabidopsis* counterparts.

Many studies show that some of the metal transport families are non-selective. The Fe transporter IRT1 is actually a universal metal transporter in both *Arabidopsis* and rice. OsIRT1 was shown to transport Fe, Cd, and Zn in rice (Lee and An, 2009). The induction of OsIRT1 by Fe deficiency mediated by the OsbHLH156–OsIRO2 TF complex should contribute to the accumulation of Mn, Cu, and Zn under Fe deficiency. In addition, OsNRAMP6 and OsHMA2 may also be the candidates for non-selective metal transport. OsNRAMP1, 3, 5, and 6 were shown to transport Fe, Cd (OsNRAMP1 and 5, Takahashi *et al.*, 2011; Ishimaru *et al.*, 2012), and Mn (OsNRAMP3 and 5, Ishimaru *et al.*, 2012; Yang *et al.*, 2013), whereas OsNRAMP6 was identified as a Fe and Mn transporter (Peris-Peris *et al.*, 2017). The heavy metal ATPase family transporter OsHMA2 was shown to transport both Fe^{2+} and Zn^{2+} (Banakar *et al.*, 2017). Thus, under Fe deficiency conditions the active OsbHLH156–OsIRO2 TF complex could directly trigger the expression of *OsNRAMP6* and *OsHMA2* (Fig. 3) and increase the accumulation of Mn, Cu, and Zn under Fe deficiency. The other direct targets OsCOPT1/7 and OsZIP5/9/10 mainly transport Cu and Zn, respectively, and attribute to the accumulation of the corresponding metal contents under Fe deficiency.

Role of the metal chelators NA and DMA on the accumulation of metal elements

The activated OsbHLH156–OsIRO2 TF complex under Fe deficiency induced expression of *OsNAS1* and *OsNAS2* and led to the increased accumulation of NA (Fig. 5A, B). NA is known as an important molecule for the translocation of Fe, Cu, and Ni the in xylem (Curie *et al.*, 2009), which can result in the accumulation of Cu, and probably Zn and Mn as well. Different from *Arabidopsis*, as a Strategy I plant, rice can use NA as a substrate to further synthesize DMA, which can be secreted into soil to chelate Fe(III). The DMA–Fe(III) complex can be transported by YSL proteins and delivered in xylem and phloem saps for long distance transportation of Fe and possibly other metals (Mori *et al.*, 1991).

Increasing the Cu supply alleviates Fe-deficiency symptoms

Cu and Fe can be alternately used as enzymes that catalyse the same biochemical reactions in many plants, depending on metal availability in multicellular organisms (Marschner, 1995; Puig *et al.*, 2007). Research has shown that Cu-related genes are regulated by Fe deficiency and Cu-containing superoxide dismutase (SODs) might replace Fe-containing SODs under Fe deficiency to scavenge reactive oxygen species (Waters *et al.*, 2012). In *Arabidopsis*, Fe deficiency induced the expression of Cu-uptake genes (*AtCOPT2*, *AtFRO4*, and *AtFRO5*)

meditated by FIT and bHLH Ib, and increased Cu accumulation (Cai *et al.*, 2021). The increase in endogenous Cu concentration favours the cofactor supply to Cu/ZnSOD, which can compensate for the decrease of Fe-containing SOD, thus enhancing plant tolerance to Fe-deficiency stress (Cai *et al.*, 2021). In this study, we found that Fe-deficiency symptoms in *osbhlh156* and *osiro2* appeared under Cu deficient conditions, but not the control conditions (Fig. 7B), implying that Cu supply could alleviate the leaf chlorosis by reducing accumulation of reactive oxygen species caused by Fe deficiency. Indeed, excess Cu supply could compensate for the Fe deficiency to some extent (Supplementary Fig. S9).

A working model of OsbHLH156/OsIRO2 in facilitating accumulation of Mn, Cu, and Zn in rice shoots

Taken together, we propose a working model for OsbHLH156 and OsIRO2 in Mn, Cu, and Zn transport in rice. Under Fe deficiency, *OsbHLH156* and *OsIRO2* are strongly induced. The higher levels of the OsbHLH156 TF could assist the entrance of OsIRO2 into the nucleus (Wang *et al.*, 2020) and then form a complex with OsIRO2 to regulate Mn, Cu, and Zn transport via multiple ways: (i) induction of Fe transporters that can also transport other divalent metals; (ii) induction of metal chelators like NA and DMA that can also chelate Mn, Cu, Zn; and (iii) gene regulation that affects the signalling pathways upstream of the uptake and translocation of Mn, Cu, and Zn (Figs 3, 4) (Rai *et al.*, 2021). Ultimately, Fe deficiency activates universal or specific metal transporters and metal chelators that cause elevated Mn, Cu, and Zn concentrations in rice.

Supplementary data

The following supplementary data are available at *JXB* online.

Fig. S1. Genotypes of the *osbhlh156* and *osiro2* mutants.

Fig. S2. Phenotypes of WT, *osbhlh156*, and *osiro2* plants under flooded and dry land conditions.

Fig. S3. Number of differently expressed genes in roots of WT, *osbhlh156*, and *osiro2* plants.

Fig. S4. Relative expression of *OsACTIN1* under different conditions.

Fig. S5. OsbHLH156 is required for nuclear localization of OsIRO2 *in vivo*. (A) Western blot. (B) Immunostaining.

Fig. S6. Time course analysis of *OsbHLH156* and *OsIRO2*.

Fig. S7. Transcriptional activation assay in yeast.

Fig. S8. Phenotypes of *osbhlh156* and *osiro2* mutant lines grown under Mn-, Cu-, or Zn-deficiency conditions.

Fig. S9. Effects of excess Cu supply on plant growth under Fe deficiency.

Table S1. List of primers used in this study.

Table S2. List of differentially expressed genes in roots.

Table S3. List of potential target genes of *OsbHLH156* or *OsIRO2*.

Table S4. FPKM values for genes involved in Fe uptake and translocation in roots of from WT, *osbhlh156*, and *osiro2* plants.

Table S5. GO enrichment analysis results of the WT and mutants.

Table S6. KEGG pathway enrichment analysis results of the WT and mutants.

Acknowledgements

The authors would like to thank BGI (Shenzhen, China) for RNA sequencing. We also thank Dr Jiming Xu and Dr Shelong Zhang for technical assistance.

Author contributions

SW and HS conceived and designed the project; SW, JZ, and JL carried out most of the experiments; XH, JW, and JF performed the elements analysis; JL analysed the RNA-seq data; SW and HS wrote the article; and all authors reviewed the manuscript.

Conflict of interest

The authors declare that there is no conflict of interest.

Funding

This work was supported by the Ministry of Science and Technology of China (2021YFF1000402) to HS, the Key Research Project of the Zhejiang Lab (2021PE0AC04), and the Young Scientists Group Project (2022QNXZ05) of Northeast Institute of Geography and Agroecology to SW.

Data availability

The RNA-seq data are available in the NCBI database under accession no. PRJNA953815. Data supporting the findings in this study are available within the paper and within its supplementary data published online.

References

Alejandro S, Holler S, Meier B, Peiter E. 2020. Manganese in plants: from acquisition to subcellular allocation. Frontiers in Plant Science 11, 300.

Arrivault S, Senger T, Krämer U. 2006. The *Arabidopsis* metal tolerance protein AtMTP3 maintains metal homeostasis by mediating Zn exclusion from the shoot under Fe deficiency and Zn oversupply. The Plant Journal 46, 861–879.

Banakar R, Alvarez Fernandez A, Abadia J, Capell T, Christou P. 2017. The expression of heterologous Fe(III) phytosiderophore transporter HvYS1 in rice increases Fe uptake, translocation and seed loading and excludes heavy metals by selective Fe transport. Plant Biotechnology Journal 15, 423–432.

Barberon M, Dubeaux G, Kolb C, Isono E, Zelazny E, Vert G. 2014. Polarization of IRON-REGULATED TRANSPORTER 1 (IRT1) to the plant-soil interface plays crucial role in metal homeostasis. Proceedings of the National Academy of Sciences, USA 111, 8293–8298.

Bashir K, Ahmad Z, Kobayashi T, Seki M, Nishizawa NK. 2021. Roles of subcellular metal homeostasis in crop improvement. Journal of Experimental Botany 72, 2083–2098.

Bashir K, Rasheed S, Kobayashi T, Seki M, Nishizawa NK. 2016. Regulating subcellular metal homeostasis: the key to crop improvement. Frontiers in Plant Science 7, 1192.

Cai Y, Li Y, Liang G. 2021. FIT and bHLH Ib transcription factors modulate iron and copper crosstalk in *Arabidopsis*. Plant, Cell & Environment 44, 1679–1691.

Cailliatte R, Schikora A, Briat JF, Mari S, Curie C. 2010. High-affinity manganese uptake by the metal transporter NRAMP1 is essential for *Arabidopsis* growth in low manganese conditions. The Plant Cell 22, 904–917.

Chen S, Jin W, Wang M, Zhang F, Zhou J, Jia Q, Wu Y, Liu F, Wu P. 2003. Distribution and characterization of over 1000 T-DNA tags in rice genome. The Plant Journal 36, 105–113.

Cheng L, Wang F, Shou H, *et al*. 2007. Mutation in nicotianamine aminotransferase stimulated the Fe(II) acquisition system and led to iron accumulation in rice. Plant Physiology 145, 1647–1657.

Cohen CK, Fox TC, Garvin DF, Kochian LV. 1998. The role of iron-deficiency stress responses in stimulating heavy-metal transport in plants. Plant Physiology 116, 1063–1072.

Connolly EL, Campbell NH, Grotz N, Prichard CL, Guerinot ML. 2003. Overexpression of the FRO2 ferric chelate reductase confers tolerance to growth on low iron and uncovers posttranscriptional control. Plant Physiology 133, 1102–1110.

Curie C, Alonso JM, Le Jean M, Ecker R, Briat JF. 2000. Involvement of NRAMP1 from *Arabidopsis thaliana* in iron transport. Biochemical Journal 347, 749–755.

Curie C, Cassin G, Couch D, Divol F, Higuchi K, Le Jean M, Misson J, Schikora A, Czernic P, Mari S. 2009. Metal movement within the plant: contribution of nicotianamine and yellow stripe 1-like transporters. Annals of Botany 103, 1–11.

Curie C, Panaviene Z, Loulergue C, Dellaporta SL, Briat JF, Walker EL. 2001. Maize yellow stripe1 encodes a membrane protein directly involved in Fe(III) uptake. Nature 409, 346–349.

Deng F, Yamaji N, Xia J, Ma JF. 2013. A member of the heavy metal P-type ATPase OsHMA5 is involved in xylem loading of copper in rice. Plant Physiology 163, 1353–1362.

Eroglu S, Meier B, von Wirén N, Peiter E. 2015. The vacuolar manganese transporter MTP8 determines tolerance to iron deficiency-induced chlorosis in *Arabidopsis*. Plant Physiology 170, 1030–1045.

Gindri RG, Navarro BB, da Cruz Dias PV, *et al*. 2020. Physiological responses of rice (*Oryza sativa* L.) *oszip7* loss-of-function plants exposed to varying Zn concentrations. Physiology and Molecular Biology of Plants 26, 1349–1359.

Grotz N, Guerinot ML. 2006. Molecular aspects of Cu, Fe and Zn homeostasis in plants. Biochimica et Biophysica Acta 1763, 595–608.

Hansch R, Mendel RR. 2009. Physiological functions of mineral micronutrients (Cu, Zn, Mn, Fe, Ni, Mo, B, Cl). Current Opinion in Plant Biology 12, 259–266.

Hao C, Yang Y, Du J, Deng XW, Lei Li L. 2022. The PCY-SAG14 phytocyanin module regulated by PIFs and miR408 promotes dark-induced leaf senescence in *Arabidopsis*. Proceedings of the National Academy of Sciences USA 119, e2116623119.

Inoue H, Higuchi K, Takahashi M, Nakanishi H, Mori S, Nishizawa NK. 2003. Three rice nicotianamine synthase genes, *OsNAS1*, *OsNAS2*, and *OsNAS3* are expressed in cells involved in long-distance transport of iron and differentially regulated by iron. The Plant Journal 36, 366–381.

Inoue H, Kobayashi T, Nozoye T, Takahashi M, Kakei Y, Suzuki K, Nakazono M, Nakanishi H, Mori S, Nishizawa NK. 2009. Rice OsYSL15 is an iron-regulated iron(III)-deoxymugineic acid transporter expressed in the roots and is essential for iron uptake in early growth of the seedlings. The Journal of Biological Chemistry 284, 3470–3479.

Ishimaru Y, Masuda H, Bashir K, *et al*. 2010. Rice metal-nicotianamine transporter, OsYSL2, is required for the long-distance transport of iron and manganese. The Plant Journal 62, 379–390.

Ishimaru Y, Masuda H, Suzuki M, Bashir K, Takahashi M, Nakanishi H, Mori S, Nishizawa NK. 2007. Overexpression of the OsZIP4 zinc transporter confers disarrangement of zinc distribution in rice plants. Journal of Experimental Botany 58, 2909–2915.

Ishimaru Y, Suzuki M, Kobayashi T, Takahashi M, Nakanishi H, Mori S, Nishizawa NK. 2005. OsZIP4, a novel zinc-regulated zinc transporter in rice. Journal of Experimental Botany 56, 3207–3214.

Ishimaru Y, Suzuki M, Tsukamoto T, *et al*. 2006. Rice plants take up iron as an Fe^{3+}-phytosiderophore and as Fe^{2+}. The Plant Journal 45, 335–346.

Ishimaru Y, Takahashi R, Bashir K, *et al*. 2012. Characterizing the role of rice NRAMP5 in manganese, iron and cadmium transport. Scientific Reports 2, 286.

Kirk GJD, Manwaring HR, Ueda Y, Semwal VK, Wissuwa M. 2022. Below-ground plant-soil interactions affecting adaptations of rice to iron toxicity. Plant, Cell & Environment 45, 705–718.

Kobayashi T, Nishizawa NK. 2012. Iron uptake, translocation, and regulation in higher plants. Annual Review of Plant Biology 63, 131–152.

Kobayashi T, Nakanishi Itai R, Nishizawa NK. 2014. Iron deficiency responses in rice roots. Rice 7, 27.

Kobayashi T, Nozoye T, Nishizawa NK. 2019. Iron transport and its regulation in plants. Free Radical Biology and Medicine 133, 11–20.

Korshunova YO, Eide D, Clark WG, Guerinot ML, Pakrasi HB. 1999. The IRT1 protein from *Arabidopsis thaliana* is a metal transporter with a broad substrate range. Plant Molecular Biology 40, 37–44.

Lee S, An G. 2009. Over-expression of *OsIRT1* leads to increased iron and zinc accumulations in rice. Plant, Cell & Environment 32, 408–416.

Liang G, Zhang H, Li Y, Pu M, Yang Y, Li C, Lu C, Xu P, Yu D. 2020. *Oryza sativa* FER-LIKE FE DEFICIENCY-INDUCED TRANSCRIPTION FACTOR (OsFIT/OsbHLH156) interacts with OsIRO2 to regulate iron homeostasis. Journal of Integrative Plant Biology 62, 668–689.

Long TA, Tsukagoshi H, Busch W, Lahner B, Salt DE, Benfey PN. 2010. The bHLH transcription factor POPEYE regulates response to iron deficiency in *Arabidopsis* roots. The Plant Cell 22, 2219–2236.

Ma JF, Nomoto K. 1993. Two related biosynthetic pathways of mugineic acids in gramineous plants. Plant Physiology 102, 373–378.

Ma JF, Shinada T, Matsuda C, Nomoto K. 1995. Biosynthesis of phytosiderophores, mugineic acids, associated with methionine cycling. The Journal of Biological Chemistry 270, 16549–16554.

Marschner H. 1995. Mineral nutrition of higher plants. 2nd edn. London: Academic Press.

Maurya S, Vishwakarma AK, Dubey M, Shrivastava P, Shrivastava R, Chandel G. 2018. Developing gene-tagged molecular marker for functional analysis of OsZIP10 metal transporter gene in rice. Indian Journal of Genetics and Plant Breeding 78, 180.

Mori S, Nishizawa N, Hayashi H, Chino M, Yoshimura E, Ishihara J. 1991. Why are young rice plants highly susceptible to iron deficiency? Plant and Soil 130, 143–156.

Morrissey J, Baxter IR, Lee J, Li L, Lahner B, Grotz N, Kaplan J, Salt DE, Guerinot ML. 2009. The ferroportin metal efflux proteins function in iron and cobalt homeostasis in *Arabidopsis*. The Plant Cell 21, 3326–3338.

Nishiyama R, Kato M, Nagata S, Yanagisawa S, Yoneyama T. 2012. Identification of Zn-nicotianamine and Fe-2'-deoxymugineic acid in the phloem sap from rice plants (*Oryza sativa* L). Plant and Cell Physiology 53, 381–390.

Nozoye T, Nagasaka S, Kobayashi T, Takahashi M, Sato Y, Sato Y, Uozumi N, Nakanishi H, Nishizawa NK. 2011. Phytosiderophore efflux transporters are crucial for iron acquisition in graminaceous plants. The Journal of Biological Chemistry 286, 5446–5454.

Ogo Y, Itai RN, Nakanishi H, Inoue H, Kobayashi T, Suzuki M, Takahashi M, Mori S, Nishizawa NK. 2006. Isolation and characterization

of IRO2, a novel iron-regulated bHLH transcription factor in graminaceous plants. Journal of Experimental Botany 57, 2867–2878.

Ogo Y, Itai RN, Nakanishi H, Kobayashi T, Takahashi M, Mori S, Nishizawa NK. 2007. The rice bHLH protein OsIRO2 is an essential regulator of the genes involved in Fe uptake under Fe-deficient conditions. The Plant Journal 51, 366–377.

Peris-Peris C, Serra-Cardona A, Sanchez-Sanuy F, Campo S, Arino J, San Segundo B. 2017. Two NRAMP6 isoforms function as iron and manganese transporters and contribute to disease resistance in rice. Molecular Plant-Microbe Interactions 30, 385–398.

Pich A, Scholz G. 1996. Translocation of copper and other micronutrients in tomato plants (*Lycopersicon esculentum* Mill): nicotianamine-stimulated copper transport in the xylem. Journal of Experimental Botany 47, 41–47.

Puig S, Andrés-Colás N, García-Molina A, Peñarrubia L. 2007. Copper and iron homeostasis in *Arabidopsis*: responses to metal deficiencies, interactions and biotechnological applications. Plant, Cell & Environment 30, 271–290.

Rai S, Singh PK, Mankotia S, Swain J, Satbhai SB. 2021. Iron homeostasis in plants and its crosstalk with copper, zinc, and manganese. Plant Stress 1, 100008.

Robinson NJ, Procter CM, Connolly EL, Guerinot ML. 1999. A ferric-chelate reductase for iron uptake from soils. Nature 397, 694–697.

Rogers EE, Eide DJ, Guerinot ML. 2000. Altered selectivity in an *Arabidopsis* metal transporter. Proceedings of the National Academy of Sciences, USA 97, 12356–12360.

Rout JR, Behera S, Keshari N, Ram SS, Bhar S, Chakraborty A, Sudarshan M, Sahoo SL. 2015. Effect of iron stress on *Withania somnifera* L: antioxidant enzyme response and nutrient elemental uptake of *in vitro* grown plants. Ecotoxicology 24, 401–413.

Saleh A, Alvarez-Venegas R, Avramova Z. 2008. An efficient chromatin immunoprecipitation (ChIP) protocol for studying histone modifications in *Arabidopsis* plants. Nature Protocols 3, 1018–1025.

Santi S, Cesco S, Varanini Z, Pinton R. 2005. Two plasma membrane H^+-ATPase genes are differentially expressed in iron-deficient cucumber plants. Plant Physiology and Biochemistry 43, 287–292.

Sasaki A, Yamaji N, Xia J, Ma JF. 2011. OsYSL6 is involved in the detoxification of excess manganese in rice. Plant Physiology 157, 1832–1840.

Sasaki A, Yamaji N, Yokosho K, Ma JF. 2012. Nramp5 is a major transporter responsible for manganese and cadmium uptake in rice. The Plant Cell 24, 2155–2167.

Schaaf G, Honsbein A, Meda AR, Kirchner S, Wipf D, von Wiren N. 2006. *AtIREG2* encodes a tonoplast transport protein involved in iron-dependent nickel detoxification in *Arabidopsis thaliana* roots. The Journal of Biological Chemistry 281, 25532–25540.

Takahashi M, Terada Y, Nakai I, Nakanishi H, Yoshimura E, Mori S, Nishizawa NK. 2003. Role of nicotianamine in the intracellular delivery of metals and plant reproductive development. The Plant Cell 15, 1263–1280.

Takahashi R, Ishimaru Y, Senoura T, Shimo H, Ishikawa S, Arao T, Nakanishi H, Nishizawa NK. 2011. The OsNRAMP1 iron transporter is involved in Cd accumulation in rice. Journal of Experimental Botany 62, 4843–4850.

Tan L, Qu M, Zhu Y, Peng C, Wang J, Gao D, Chen C. 2020. ZINC TRANSPORTER5 and ZINC TRANSPORTER9 function synergistically in zinc/cadmium uptake. Plant Physiology 183, 1235–1249.

Thomine S, Wang R, Ward JM, Crawford NM, Schroeder JI. 2000. Cadmium and iron transport by members of a plant transporter gene family in *Arabidopsis* with homology to *NRAMP* genes. Proceedings of the National Academy, USA 97, 4991–4996.

Ueno D, Sasaki A, Yamaji N, *et al*. 2015. A polarly localized transporter for efficient manganese uptake in rice. Nature Plants 1, 15170.

Vert G, Grotz N, Dedaldechamp F, Gaymard F, Guerinot ML, Briat JF, Curie C. 2002. IRT1, an *Arabidopsis* transporter essential for iron uptake from the soil and for plant growth. The Plant Cell 14, 1223–1233.

Wang S, Li L, Ying Y, Wang J, Shao JF, Yamaji N, Whelan J, Ma JF, Shou H. 2020. A transcription factor OsbHLH156 regulates Strategy II iron acquisition through localising IRO2 to the nucleus in rice. New Phytologist 225, 1247–1260.

Waters BM, McInturf SA, Stein RJ. 2012. Rosette iron deficiency transcript and microRNA profiling reveals links between copper and iron homeostasis in *Arabidopsis thaliana*. Journal of Experimental Botany 63, 5903–5918.

Welch RM, Norvell WA, Schaefer SC, Shaff JE, Kochian LV. 1993. Induction of iron(III) and copper(II) reduction in pea (*Pisum sativum* L) roots by Fe and Cu status: Does the root-cell plasmalemma Fe(III)-chelate reductase perform a general role in regulating cation uptake? Planta 190, 555–556.

Yamaji N, Xia J, Mitani-Ueno N, Yokosho K, Feng Ma J. 2013. Preferential delivery of zinc to developing tissues in rice is mediated by P-type heavy metal ATPase OsHMA2. Plant Physiology 162, 927–939.

Yang M, Zhang W, Dong H, Zhang Y, Lv K, Wang D, Lian X. 2013. OsNRAMP3 is a vascular bundles-specific manganese transporter that is responsible for manganese distribution in rice. PLoS One 8, e83990.

Ying Y, Yue W, Wang S, Li S, Wang M, Zhao Y, Wang C, Mao C, Whelan J, Shou H. 2017. Two h-type thioredoxins interact with the E2 ubiquitin conjugase PHO2 to fine-tune phosphate homeostasis in rice. Plant Physiology 173, 812–824.

Yuan M, Li X, Xiao J, Wang S. 2011. Molecular and functional analyses of COPT/Ctr-type copper transporter-like gene family in rice. BMC Plant Biology 11, 69.

Yuan Y, Wu H, Wang N, Li J, Zhao W, Du J, Wang D, Ling HQ. 2008. FIT interacts with AtbHLH38 and AtbHLH39 in regulating iron uptake gene expression for iron homeostasis in *Arabidopsis*. Cell Research 18, 385–397.

Zahra N, Hafeez MB, Shaukat K, Wahid A, Hasanuzzaman M. 2021. Fe toxicity in plants: impacts and remediation. Physiologia Plantarum 173, 201–222.

Zhao H, Wu L, Chai T, Zhang Y, Tan J, Ma S. 2012. The effects of copper, manganese and zinc on plant growth and elemental accumulation in the manganese-hyperaccumulator *Phytolacca americana*. Journal of Plant Physiology 169, 1243–1252.

Zheng L, Yamaji N, Yokosho K, Ma JF. 2012. YSL16 is a phloem-localized transporter of the copper-nicotianamine complex that is responsible for copper distribution in rice. The Plant Cell 24, 3767–3782.